

# Repurposing Templates for Zeolite Synthesis from Simulations and Data Mining

Daniel Schwalbe-Koda, Omar A. Santiago-Reyes, Avelino Corma, Yuriy Román-Leshkov, Manuel Moliner, and Rafael Gómez-Bombarelli\*



Cite This: *Chem. Mater.* 2022, 34, 5366–5376



Read Online

ACCESS |



Metrics & More

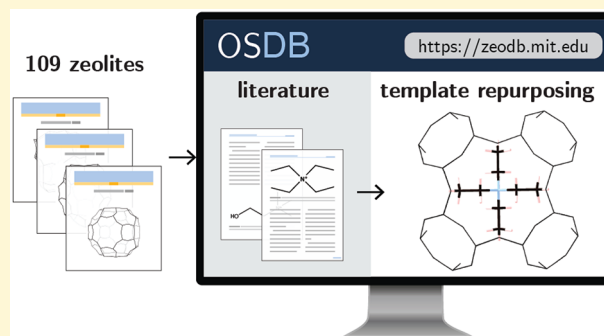


Article Recommendations



Supporting Information

**ABSTRACT:** Zeolites span a large variety of microporous crystal structures, making them useful materials for catalysis and separations. However, controlling phase competition in their synthesis often requires organic structure-directing agents (OSDAs) to selectively crystallize the desired topologies. Whereas computational design of OSDAs can help in selecting adequate candidates for zeolite synthesis, machine-generated templates are often complex or expensive. In this work, we use shape and binding metrics to propose templates for over 100 zeolites and to rationalize dual-OSDA approaches. Starting from OSDAs from the literature, promising templates were selected for zeolites ranging from clathrasil frameworks to extra large-pore structures. Selectivity maps derived from phase competition metrics show that small- and medium-pore zeolites tend to be more shape-selective toward their templates than their large-pore counterparts. Finally, shape and volume descriptors allow identification of OSDAs that may act as synergistic pore-fillers for different cavities of zeolites. The application of this theory is demonstrated for the case of the KFI zeolite, which may be synthesized using tetraethylammonium and OSDAs repurposed from high-silica LTA synthesis as dual OSDAs. This work may help in the discovery of new synthesis routes for known zeolites using shape descriptors and repurposed OSDAs.



## INTRODUCTION

Zeolites are nanoporous materials with a myriad of applications in industrial catalysis and separations<sup>1–3</sup> and hold promise for sustainable processes.<sup>4</sup> The variety of synthetically accessible zeolite polymorphs enables confinement and transport effects to be tuned.<sup>5</sup> This topological diversity derives from strong phase competition between metastable zeolite structures, and it must be controlled to tailor shape selectivity toward molecular recognition or catalysis.<sup>6–8</sup> However, designing synthesis routes toward a target zeolite topology is a labor-intensive task. Zeolites are typically crystallized in hydrothermal conditions, where inorganic precursors and organic templates cooperate to synthesize a topology.<sup>9,10</sup> Due to this high-dimensional synthetic parameter space, finding cost-effective and selective routes to synthesize zeolites has been the focus of research works for decades. Within the hydrothermal synthesis of zeolites, organic structure-directing agents (OSDAs) play an important role in crystallizing certain topologies.<sup>5,11</sup> A combination of electrostatic and dispersion interactions drives the nucleation of topologies that act as good hosts for that template,<sup>10</sup> with the dispersion interaction often determining the outcome topology.<sup>11</sup> Although OSDA-free synthesis routes are possible,<sup>12–16</sup> they are often limited in terms of selectivity or in the compositions of the final product. On the other hand,

OSDA-based routes can yield high-silica zeolites with a variety of topologies upon the adequate choice of an OSDA.<sup>17</sup>

Computational methods can aid the design of organic templates prior to experimentation.<sup>18–25</sup> However, since most computational methods usually predict molecules for one framework at a time, they are unable to predict competing phases that could also be crystallized by the given molecule. We recently tackled this problem by quantifying phase selectivity in zeolite synthesis using over half a million simulations, literature mining,<sup>25,26</sup> and experimental validation.<sup>27,28</sup> It was demonstrated that selectivity metrics based on binding energies and on shape-matching are important in template-based zeolite synthesis, enabling a computational screening of OSDAs for zeolites. Nevertheless, selectivity is not the only design metric for OSDAs. In order to be practically useful, computer-designed OSDAs must be simultaneously selective and chemically realizable. Although strategies like rule-based molecular enumeration<sup>29,30</sup> and computational

Received: January 7, 2022

Revised: May 25, 2022

Published: June 14, 2022



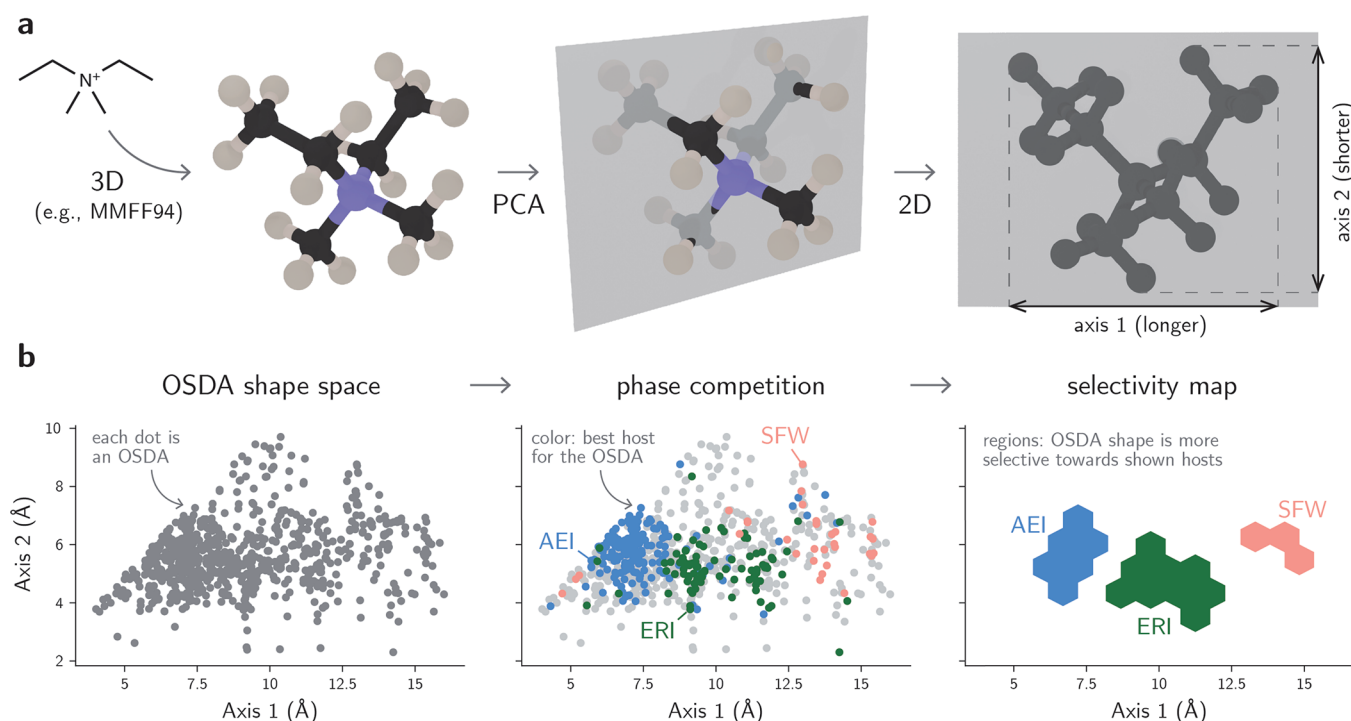


**Figure 1.** a, Diagram to calculate the shape of an OSDA using two principal axes. The 3D coordinates of the conformer are projected onto a two-dimensional plane, from which the axes are obtained. b, Construction of a shape selectivity map. Regions of the OSDA shape space are colored according to the strongest binding host toward each template within the systems under analysis.

retrosynthesis<sup>20,24</sup> can aid the exploration of synthesizable chemical spaces or automatically suggest synthesis routes for novel OSDAs, inventing novel molecules *in silico* may require expensive synthesis routes for production.<sup>24,31</sup>

To disentangle these issues of “chemical feasibility” of generated molecules from the computational templating metrics, we focus on proposing known templates from the literature to obtain zeolites that have not been realized with those OSDAs. In the pharmaceutical field, this strategy of employing known drugs toward new applications is known as drug repurposing or repositioning and is used as a way to reduce the time-to-market of new drugs, since molecules are already validated to be safe and have good physicochemical and toxicological profiles.<sup>32</sup> This analogue strategy for OSDA design may offer several advantages, including the following: (i) bypassing the need to design new OSDAs that are simultaneously stable and soluble in hydrothermal conditions, (ii) avoiding the design of new synthesis routes for the molecules, and (iii) enabling a faster adoption of new zeolite synthesis routes in industrial applications by relying on known templates. In this work, we combine descriptor analysis and data mining to repurpose known OSDAs for zeolites. Studying from clathrasils to extra large-pore zeolites, we analyze how OSDA volume and shape control phase competition metrics in over 100 zeolites. In particular, the following contributions are put forward:

1. Introducing shape selectivity maps from computational metrics, providing insights on how molecular shape influences binding energies in zeolites.
2. Repurposing OSDAs for over 100 known zeolites using shape and binding metrics
3. Rationalizing the design of dual-OSDA routes for zeolites using shape metrics, as exemplified by the LTA and KFI zeolites.

This work provides a comprehensive theoretical analysis on shape selectivity for zeolites. The multiple opportunities shown here may guide future experiments toward zeolite discovery and OSDA repurposing.

## METHODS

**Binding Energy Data.** The simulation data was obtained from ref 28, where all simulation details are discussed in-depth. Initial zeolite structures were downloaded from the International Zeolite Association (IZA) database<sup>33</sup> and preoptimized using the Sanders-Leslie-Catlow (SLC) parametrization.<sup>34</sup> The preoptimization is useful to systematize the structures according to a level of theory that can be extended toward nonexperimental zeolites.<sup>35</sup> Conformers for OSDAs were generated using RDKit<sup>36</sup> with the MMFF94 force field.<sup>37,38</sup>

OSDA-zeolite poses were generated using Voronoi and Monte Carlo docking algorithms in the VOID package.<sup>39</sup> Up to five different conformers for each OSDA were used as input geometries for VOID. As the occluded molecular conformation can change depending on the outcome zeolite,<sup>40,41</sup> the use of different rigid conformers during docking increases the diversity of poses obtained by the algorithm. The Voronoi docking algorithm used the default parameters described in ref 39, with threshold fitness function with minimum distance of 1.25 Å, five k-means clusters of Voronoi nodes generated with at least 3 Å of radius, and a probe radius of 0.1 Å. The Monte Carlo docker algorithm uses 1,000 Monte Carlo steps with a normalized temperature of 0.1 for the first 500 steps and 0.0 for the last 500 steps. Although the docking algorithms are run until the loading of OSDAs in zeolites is maximized, the three largest OSDA loadings are simulated downstream using force field calculations. The final pose is the one that minimizes the overall energy of the system among the simulated structures, including guest-guest interactions. This “variational” approach to binding energy was successful in recalling the outcomes of zeolite synthesis from the literature.<sup>28</sup>

Force field calculations were performed using the General Utility Lattice Program (GULP) version 5.1.1<sup>42,43</sup> through the GULPy package.<sup>35</sup> The Dreiding force field<sup>44</sup> was used to model dispersion interactions between pure-silica zeolites and OSDAs. Despite the

absence of electrostatic interactions, this approach has demonstrated good agreement when quantifying phase competition from the literature<sup>28</sup> and reasonable correlation with density functional theory calculations.<sup>35</sup> Binding energies between zeolites and OSDAs were computed using the frozen pose method, where the host–guest interaction energy is obtained after optimizing the systems at constant volume.<sup>35</sup>

The binding energy between a zeolite and an OSDA can be quantified using different normalizations, such as normalization per SiO<sub>2</sub> or OSDA. The normalizations provide different interpretations toward OSDA design and can help in comparing frameworks with distinct building units.<sup>28</sup> When binding energies are compared for a single OSDA across different zeolites, a new metric called “competition energy” is defined. This metric ranks different hosts toward a certain template according to their strength of binding. We adopt the convention that lower competition energies indicate a more preferential binding toward a particular framework using the second-best host as the zero reference for this competition energy.

**Volume and Shape Descriptors.** The volume of the OSDA was calculated using a voxel-based approach. The lowest-energy conformer, as calculated by the MMFF94 force field (see section above), is chosen as the reference geometry. Then, the molecular volume is quantified using a grid of 0.2 Å and a margin of 2.0 Å for the boxes enclosing the conformer, as implemented in RDKit.<sup>36</sup>

In volume-energy visualizations, each OSDA was represented with a marker. If the OSDA was known to synthesize a particular framework, the data point was depicted with a triangle. Otherwise, the data point was depicted with a circle. OSDAs selected as promising candidates for repurposing (see the **OSDA Selection** section below) were highlighted with squares whenever they have not been used, to our knowledge, to synthesize the framework under study.

OSDA shape descriptors were calculated by reducing the dimensionality of the nuclear coordinates into a 2D space based on a principal component analysis (PCA) of the molecular conformer.<sup>28</sup> The procedure for calculating the shape metric is the following (see also **Figure 1a**):

1. The 3D molecular conformer is calculated using simulation methods.
2. A 2D plane is fitted to the 3D molecular coordinates in order to maximize the explained variance of this distribution of 3D points into the projected 2D space. This is equivalent to performing a PCA-based dimensionality reduction of the 3D atomic positions toward a 2D space.
3. Onto the projected plane, the range of projected coordinates is computed.

Thus, the shape descriptor enables a 3D geometry to be mapped to two principal axes, with axis 1 being the larger component. Despite the simplicity of this representation, it has been shown to correlate with synthetic accessibility of zeolites in OSDA design.<sup>28</sup>

In shape-energy visualizations, the shape space of OSDAs—as described by the two principal axes of the molecule—is discretized in hexagonal bins. Each bin is colored using the average binding or competition energy of all OSDAs falling within that region. Brighter colors indicate that OSDAs sharing that shape are, on average, stronger binders to the framework than regions with darker colors. Although changing the parameters of hexagonal binning affect the final visualization, features such as energy minima are preserved in this shape selectivity graph, enabling their qualitative interpretation.

**Selectivity Map.** A selectivity map for a family of zeolites is created by first plotting all OSDAs onto the shape space using the two-dimensional metric described above (**Figure 1b**). Then, for each OSDA, zeolites are ranked according to their binding energy. The zeolite with the lowest binding energy (most competitive phase) toward each OSDA is highlighted in the shape space of templates with a different color. Finally, a map is then obtained by binning the number of OSDAs in a given region of the shape space and discretizing these bins according to the most representative zeolite in that region. In some cases where more than one zeolite dominates a given region, both frameworks are shown with overlapping bins. In

other cases, outliers in the shape space are omitted to improve the clarity of the visualization (see **Figure 1b**). Due to the qualitative nature of this plot, selectivity maps should be interpreted as a tool to build intuition on how molecular shape affects zeolite selectivity. Whereas the overall appearance of the plot would change with different binning parameters, the outcome remains helpful not only for repurposing strategies but also for identifying regions of OSDA biselectivity for intergrowths.<sup>27,45</sup>

The selectivity map is performed within families of zeolites, i.e., groups of frameworks sharing the same maximum ring size. Although phase competition is not limited to zeolites with similar ring sizes—that is, a large-pore zeolite such as Beta can be the outcome of a synthesis targeting a small-pore framework—the shape space of similar structures can be best interpreted when families are compared. In addition, the selectivity map is a qualitative assessment of the shape space of the zeolites and is limited by the representation power of the two-dimensional descriptor. Nevertheless, it is a useful tool to visualize shape selectivity in zeolites, aiding interpretability to the simulation results.

**OSDA Selection.** OSDAs were downselected according to their volume, shape, synthetic complexity, and binding metrics using OSDDB.<sup>28</sup> In particular, the data available at OSDDB was explored using expert knowledge to select OSDAs for the synthesis of each zeolite. Whereas synthetic complexity metrics can be used for OSDA design,<sup>28</sup> the interactive visualizations further aid expert-based selection of molecules with higher potential and/or lower cost.

In addition to expert-based synthetic complexity, the following heuristic rules for downselection were imposed to restrict the search space:

- Positively charged OSDAs were preferred over neutral ones, motivated by the synthesis of aluminosilicate zeolite structures over zeotypes.
- Phosphonium-based OSDAs were less preferred due to restrictions related to the industrial application of such templates.
- Templates with hydroxyl groups were less favored due to their reduced hydrothermal stability.

Despite these requirements, no OSDAs were removed from the volume-energy plots for compatibility with the public interface implemented in OSDDB.

OSDA selection was performed by first identifying preferential volumes of OSDAs toward a particular zeolite by exploring the regions near energy minima in volume-energy plots. Whenever zeolites have more than one energy minimum, OSDAs in all minima were investigated. Although molecules with volumes smaller than 175 Å can seemingly lead to strong binding energies, particularly in large- and extra large-pore zeolites, they often require higher loadings to achieve such low energies. Smaller sizes and higher loadings may increase the competition energy of the templates, thus making them less selective for larger structures.<sup>28</sup> Therefore, promising OSDAs were identified by simultaneously maximizing the binding strength and volume within the constraints described above.

After OSDAs with volumes of interest were downselected, the molecules were compared according to their shapes. If the shape space of the zeolite exhibits regions of higher selectivity, i.e., shapes that lead to lower average energies, OSDAs exhibiting shapes leading to these energy minima were preferred over templates with distinct shapes. This shape-driven downselection of molecules has demonstrated an increase in the synthetic accessibility of zeolites.<sup>28</sup> On the other hand, if the zeolite framework does not exhibit local minima in the energy-shape landscape, molecules with diverse shapes are proposed.

## RESULTS AND DISCUSSION

**Six-Membered Ring Zeolites.** Zero-dimensional zeolites are examples of systems where, at a constant gel composition, the choice of the OSDA often determines the outcome of the synthesis.<sup>11</sup> Six-membered frameworks are considered inacces-

sible for the diffusion of molecules and thus are rarely sought to be synthesized with OSDAs. However, their constituent building units are sometimes observed in other zeolites. Thus, analyzing structure-directing effects in zero-dimensional zeolites is essential not only to control phase competition effects but also to understand how to direct the formation of particular building units shared between these and other zeolites.

Figures S1–S12 show examples of OSDAs that are known to lead to the synthesis of zero-dimensional zeolite structures. In many cases, the templates are small, such as the ones for the SOD zeolite (Figure S9). The *sod* building unit is selectively synthesized using tetramethylammonium or similar small molecules. Although synthesizing the SOD framework is typically undesirable, understanding the shape selectivity of its components can guide the synthesis of zeolites with more interesting applications such as LTA. In other cases, zeolites with larger volumes such as NON (Figure S6) or SGT (Figure S8) may compete with the synthesis of small-pore frameworks. In particular, spiro-type OSDAs show similar binding patterns between NON and CHA zeolites, and synthesis routes involving these OSDAs may result in NON or LOS (Figure S4) frameworks rather than the more commercially interesting CHA framework.<sup>28</sup> Finally, longer or wider OSDAs may crystallize zero-dimensional zeolites with large cavities such as LIO (Figure S3), MSO (Figure S5), TOL (Figure S11), or UOZ (Figure S12). As directing the crystallization of substructures in these frameworks is often undesirable, the phase competition analysis allows the avoidance of templates which may lead to these zeolites rather than targeted ones.

**Small-Pore Zeolites.** Small-pore zeolites are characterized by cavities with eight-membered rings. The confinement effects due to the cavity sizes and shapes are responsible for altering catalyst stability and selectivity for many chemical processes, including selective catalytic reduction of NO<sub>x</sub> or methanol-to-olefin reactions.<sup>46,47</sup> Modulating the shapes of OSDAs while keeping the reaction conditions constant may lead to the crystallization of different small-pore zeolites or intergrowths.<sup>28</sup> In some cases, however, frameworks such as ITE and RTH exhibit stark structural similarities,<sup>45</sup> which may hinder the control of phase competition.

Figure 2 shows a selectivity map of OSDA shapes in small-pore zeolites. The selectivity map was created by selecting the best small-pore framework toward each of the OSDAs in the database and outlining the regions of the shape space that favor each framework. The shape and binding energy metrics recover intuitive building schemes from the zeolites. For example, the LEV zeolite has the smallest cavity, and its OSDA selectivity region is found in the lower left of the shape space. On the other hand, SFW and SWY have long cages, which leads to a long axis 1 in Figure 2 but axis 2 comparable to those of AEI or RTH zeolites. In addition, the CHA/AEI regions intersect in terms of selectivity, as expected by the crystallization of these intergrown structures with biselective OSDAs. In the central region of Figure 2, the ERI zeolite has a slightly longer cage than CHA but still smaller than AFX. The LTA zeolite is an exception to these zeolites, as its large *lta* cage requires large molecules that can effectively occupy its volume in both axes.

As an example of how novel molecules can be proposed toward the synthesis of zeolites with few examples of templates in the literature, Figure 3 shows OSDAs predicted to be favorable toward the SWY zeolite. According to the selectivity

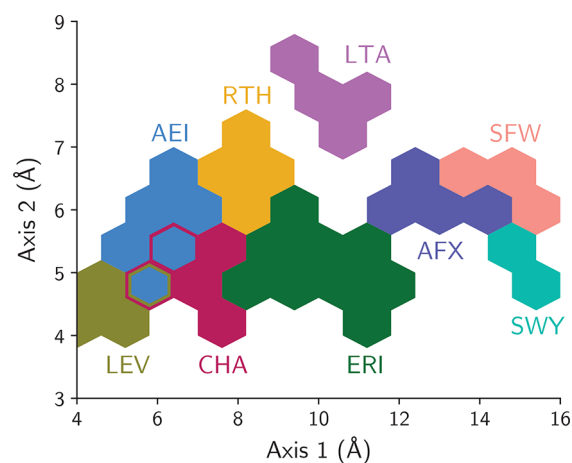


**Figure 2.** Selectivity map of OSDAs toward small-pore zeolites. Hexagons are regions of the shape space dominated by one of the frameworks, as shown in Figure 1.

map of Figure 2, OSDAs favorable toward SWY should have a shape characterized by axis 1 between 14 and 16 Å and axis 2 of about 5 Å. Indeed, the two OSDAs known to synthesize SWY, shown in Figure 3a (OSDAs 1, 2), fall within this region of the shape space. Two repurposed OSDAs (OSDAs 3 and 4 in Figure 3a) have similar shapes (Figure 3c), with cyclohexyl groups that could lower the cost of the OSDA compared to more expensive moieties such as DABCO or quinuclidine. Both OSDAs are also close to the ideal volume of ~350 Å<sup>3</sup> of the large cavity characteristic to SWY (Figure 3b). However, the binding energy and volume metrics suggest the possibility of synthesizing this zeolite with smaller OSDAs, which could assemble in pairs to fill the cavity, similarly to what is carried out in the SFW zeolite.<sup>48</sup> OSDA 5 in Figure 3a has approximately half of the volume of the cavity and is also evidenced by a minimum of binding energy in the binding-volume plots (Figure 3b). Additionally, OSDA 5 has axis 2 comparable to those from known OSDAs, indicating its adequate diameter toward the characteristic cavity of SFW, and approximately half of their length (Figure 3c). These results suggest that the proposed OSDA is an interesting candidate to attempt the synthesis of SWY.

Figures S13–39 show other examples of OSDAs from the literature predicted to be favorable toward small-pore zeolites. In addition to well-known frameworks, the figures show opportunities to attempt the crystallization of known small-pore zeolites, but with broader compositions, including the AVL (Figure S17) or SAV (Figure S36) frameworks. The figures also highlight the shape matching landscape of the following: small-cage frameworks such as ITE (Figure S25) or RTH (Figure S33); 1D channel zeolites such as AWW (Figure S18), IRN (Figure S24), or SAS (Figure S34); or structures with larger cavities such as AFX (Figure S15), EEI (Figure S20), or SAT (Figure S35).

**Medium-Pore Zeolites.** Medium-pore zeolites are widely used in petrochemical and fine-chemical applications. Zeolite ZSM-5 (MFI), for example, is a versatile material used in a variety of catalytic applications such as oil refining or xylene isomerization.<sup>49–51</sup> As another example, Theta-1 (TON) is used in paraffin isomerizations.<sup>52</sup> While ten-membered channels enable longer templates to be used in the synthesis of medium-pore zeolites, matching medium pores with molecular sizes/shapes is paramount to achieve high selectivity

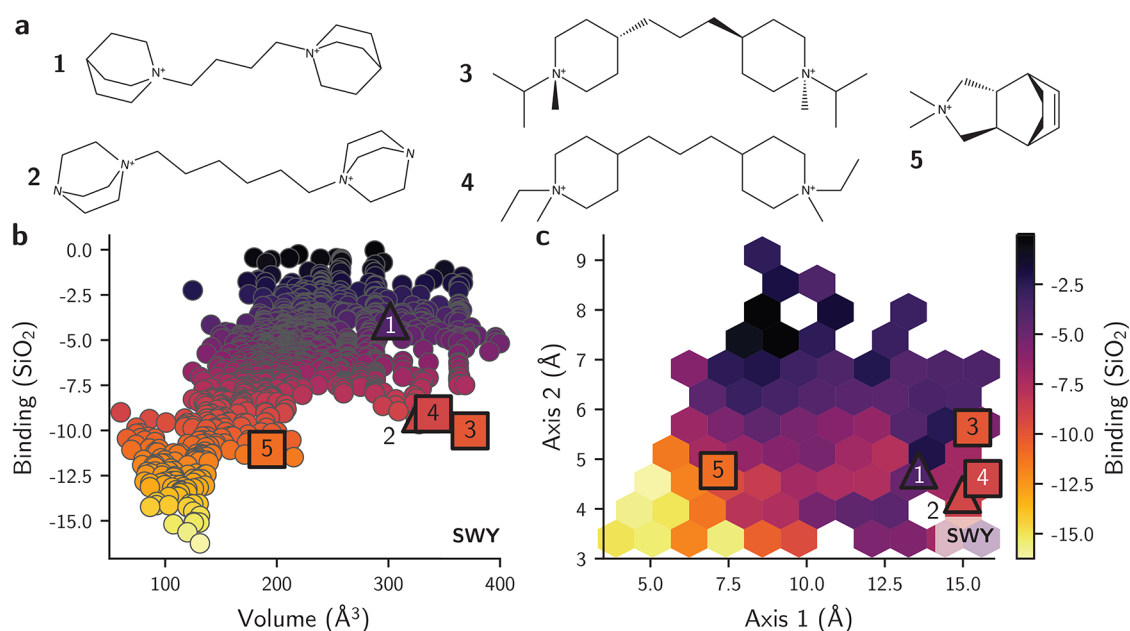


**Figure 3.** a, Known and proposed OSDAs for the synthesis of small-pore zeolite SWY. These molecules have favorable b, volume and c, shape for the synthesis of SWY. Triangles indicate OSDAs known to synthesize SWY, squares are OSDAs proposed to synthesize SWY, and circles are others.

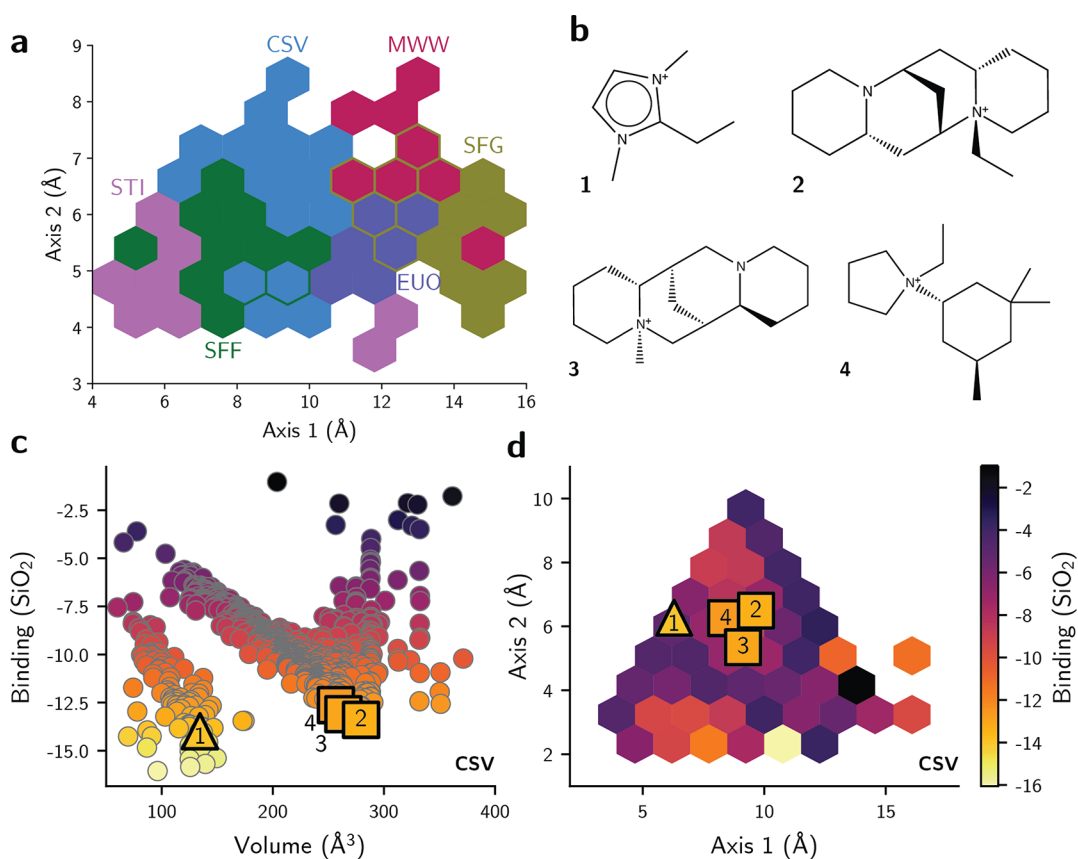


**Figure 4.** a, Selectivity map of OSDAs toward medium-pore zeolites. b, OSDAs known and proposed for the synthesis of CSV. These molecules exhibit favorable c, volume and d, shape toward this framework.

in the synthesis of these materials. Furthermore, although templates for the synthesis of some of these materials are well-known, synthesizing uncommon medium-pore frameworks with known templates can enable novel uses in catalytic applications.

Figure 4a shows the shape selectivity of OSDAs toward selected frameworks, created using the methodology described in the previous section. Different from small-pore zeolites, however, the pores of medium-pore zeolites enable templates of different sizes to be occluded within the structure, thus exhibiting lower shape selectivity. Nevertheless, frameworks

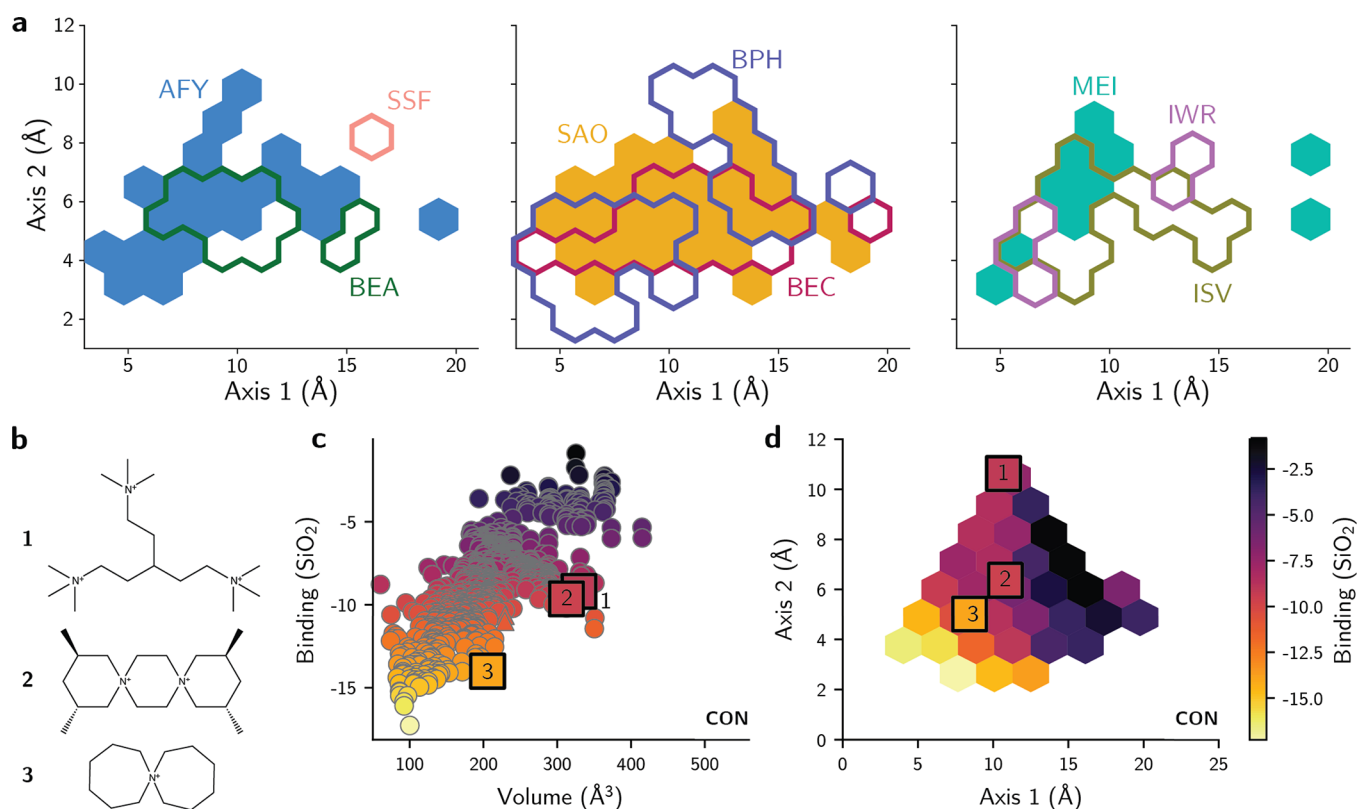


**Figure 5.** a, Selectivity map of OSDAs colored according to the best host among large-pore zeolites. Only a subset of large-pore zeolites is shown for clarity. b, OSDAs known and proposed for the synthesis of CON. These molecules exhibit c, favorable volume toward this framework. As with other large-pore zeolites, d, the shape selectivity of CON is not as distinguishable as that from small- or medium-pore zeolites.

such as STI, CSV, or MWW (Figure 4a) exhibit cavities that favor certain templates over others. In cases such as SFF or EUO (Figure 4a), the undulated pores or side pockets, respectively, may be responsible for the shape selectivity of some zeolites within templated synthesis. Finally, zeolites with intersecting pores such as SFG may be favored by larger molecules, which better occupy the large space in the pore intersection and give it higher shape selectivity compared to other medium-pore frameworks. Similar to Figure 2, Figure 4a depicts the selectivity maps for some medium-pore zeolites. This map allows the interpretation of the results of the binding metrics using the molecular shape descriptor. For instance, STI can be synthesized either with small molecules such as tetraethylammonium or with diquaternary molecules twice as long as these templates, indicating its appearance both at values of axis 1 close to 6 and 12 Å. Similarly, selectivity toward MWW and SFG increases as the size of the molecule also increases. The wide, yet short cavities of CSV favor templates with larger values of axis 2, while the side pockets of EUO favor molecules with more elongated shapes.

Figures S40–S65 show examples of OSDAs from the literature whose volumes and shapes approach ideal values for medium-pore zeolites, as derived from simulation results. In addition to the structures shown in Figure 4a, other “cage-like” zeolite structures that display clear shape selectivity toward OSDAs, as evidenced by volumes and shapes that optimize the binding energy, include EWS (Figure S45) or IFW (Figure S47). One-dimensional, medium-pore zeolites such as MTT (Figure S55) or STF (Figure S60) also exhibit binding curves with shape selectivity due to the commensurability of the OSDAs with respect to the unit cell<sup>45</sup> or the undulation of the

pore. To exemplify how OSDAs can be repurposed for the synthesis of zeolites recently discovered, thus with few known synthesis routes, we selected the example of the CSV zeolite. This framework has been discovered with the use of a diquaternary imidazolium-based OSDA and can also be synthesized using 2-ethyl-1,3-dimethylimidazolium (see 1 in Figure 4b).<sup>53</sup> The selectivity of OSDAs for this zeolite is demonstrated by the minimum of binding energy for molecules with about 140 Å<sup>3</sup> of volume, when two OSDAs occupy the main CSV cage, and around 280 Å<sup>3</sup>, when only one OSDA can occupy this same cavity. Figure 4b shows three repurposed OSDAs with volumes close to the ideal 280 Å<sup>3</sup> per cavity (Figure 4c). In particular, the sparteinium-based molecules can be prepared with one or two quaternary nitrogens, which can be an advantage if two positive charges per cage are necessary to stabilize the CSV framework. In addition, these molecules lie around a minimum of binding energy in the shape space, as evidenced by the appearance of a brighter area in Figure 4d. Therefore, the data-driven analysis proposes OSDAs 2–4 from Figure 4b as novel candidates for the synthesis of CSV zeolites.

**Large-Pore Zeolites.** Large-pore zeolites make the most of the synthetic zeolite market and are dominated mostly by frameworks such as FAU, Beta, or MOR. The large cavities and pores enable these materials to be used not only for cracking or catalytic upgrading of larger hydrocarbons but also for processing biomass-based chemicals.<sup>50</sup> One of the main challenges in the synthesis of large-pore zeolites is obtaining high Si/Al ratios required in several catalytic processes. While OSDAs can help in achieving high quality zeolites, designing templates that selectively direct the crystallization of large-pore

zeolites can be challenging. Figure 5a shows the shape selectivity diagram for a few zeolites. Contrary to small- and medium-pore zeolites, large-pore frameworks do not exhibit the same distinct shape selectivity. Although the confinement effects of each framework are system-specific, binding energies may vary substantially according to the template and may not always be ascribed to its shape. As a result, domains of shape selectivity are not as clearly observed as in Figure 2 or Figure 4.

Despite the absence of well-defined domains where OSDAs are selective toward mostly one large-pore framework, the design of templates based on shape and volume can still be performed for these zeolites. Figure 5b shows an example of OSDAs repurposed for the CIT-1 (CON) zeolite. This framework contains 12-ring channels intersecting 10-ring channels at nonperpendicular angles. Due to this unique structure, the crystallization of this framework has been realized mostly with complex OSDAs, some of which may form molecular aggregates to fill the intersections accordingly. Nevertheless, Figure 5c shows that other OSDAs may be effective toward the synthesis of this framework. In particular, the trisquaternary OSDA 1 in Figure 5b fits well into the angled pore intersection due to its flexibility and distinct shape. OSDA 2 has volume and binding energy similar to OSDA 1 yet exhibits no rotatable bonds. Instead of occupying both channels in the intersection, OSDA 2 achieves high binding strength by occupying the 10-ring channel. Similarly, OSDA 3 fills this channel with a larger loading due to its smaller volume yet shape comparable to OSDA 2 (Figure 5d), decreasing the binding energy even more. This template is similar to the OSDA proposed by Okubo et al. when cost-aware molecular generation algorithms are employed<sup>24</sup> but has a higher volume and thus may have a better pore-filling ability. Nevertheless, despite the local binding energy minimum around OSDA volumes of 200 Å<sup>3</sup> for the CON zeolite, it is unclear whether the framework can be synthesized using smaller molecules such as OSDA 3.

Figures S66–S99 showcase selected OSDAs with favorable volumes and shapes for the synthesis of large-pore zeolites. Frameworks of interest which could be synthesized using repurposed OSDAs include BEA (Figure S70), BEC (Figure S71), BOG (Figure S72), GME (Figure S78), ISV (Figure S79), or LTL (Figure S84). Given the nature of the large pores and cavities, all these zeolites could require rather large OSDAs to achieve high silicon to aluminum ratios. Frameworks with cavity-like substructures such as IWS (Figure S82), MEI (Figure S86), or MOZ (Figure S88) generally display higher shape selectivity, as supported by the binding patterns emerging from volumes and shapes of OSDAs docked in the frameworks. Structures for which few OSDAs are known, such as SSF (Figure S70), could find new practical applications if lower-cost synthesis routes were enabled by new templates. Furthermore, structures synthesized only as zeotypes such as SFO (Figure S95) may be realized with selective OSDAs that could enable their synthesis as aluminosilicates. In summary, although large-pore zeolites are not as shape-selective as their small- or medium-pore counterparts, OSDAs may still be proposed for them using binding energies, volume, and shape as interpretable design metrics.

**Extra Large-Pore Zeolites.** Beyond large-pore zeolites, structures containing rings of size larger than 12 framework sites are called extra large-pore zeolites. Their well-defined crystallinity and active site distributions contrast with mesoporous materials, making extra large-pore zeolites

potential candidates for shape-selective catalysis.<sup>54,55</sup> However, synthesizing extra large-pore zeolites exhibiting thermal stability, adequate acidity, and low cost is challenging.<sup>56,57</sup> Often, extra large-pore frameworks are synthesized as zeotypes or germanosilicates or require expensive OSDAs to be produced.<sup>55</sup>

Given the aperture sizes in these structures and the lead from large-pore zeolites, shape selectivity in these frameworks may not be achieved in the same way as small- or medium-pore zeolites. Rather, the tendency to form molecular aggregates to occupy the void space in zeolites may not be fully predicted by simulations.<sup>28</sup> Nevertheless, a few selected zeolites exhibit binding energy minima in volume plots, suggesting that certain molecular volumes and shapes can increase the binding strength by maximizing the pore-filling effects through control of loading. Figures S100–S109 show a few examples of binding energy plots and OSDAs selected for extra large-pore frameworks. Zeolites such as OSO (Figure S105) exhibit distinct shape selectivity, with a narrow range of OSDA volumes leading to low binding energies, although it may require beryllium to be synthesized. Structures such as CFI (Figure S101), SFH (Figure S106), and SFN (Figure S107) show a minimum in energy for a given volume, although this may be related to the short lengths of the unit cell parameter in the pore direction. Frameworks such as IRR (Figure S103), ITT (Figure S104), or VFI (Figure S109) have broad pores and cavities, enabling higher loadings of small molecules that minimize the overall binding energy per SiO<sub>2</sub>, although the structure-directing role of heteroatoms may play a more important role in these frameworks than the OSDA alone.<sup>55</sup> In zeolites such as VFI, large templates such as OSDA 2 in Figure S109 can have low phase competition toward the extra large-pore zeolite despite not forming molecular aggregates. This stems from the impossibility of docking larger templates into zeolites with smaller cavities or pores, thus reducing phase competition effects in OSDA-based synthesis. Finally, frameworks such as CTH (Figure S102) and UTL (Figure S108) show two distinct energy minima, corresponding to the different sizes of intersecting two-dimensional pores. Although the synthesis of extra large-pore zeolites may depend on factors beyond OSDAs, the design principles from volume matching may help in choosing adequate pore-fillers to realize these frameworks, whose diversity is still limited in the field.

**Dual-OSDA Design.** In addition to designing single OSDAs to one framework as before, the shape-based OSDA descriptors can aid the selection of templates for dual-OSDA approaches. While in several cases the use of multiple templates to synthesize a particular zeolite is undesirable due to added synthesis costs, as in the case of intergrowth structures,<sup>28,45</sup> in many other examples the approach can enable synthesizing structures with previously unattainable compositions. One of the most common cases in the literature is the synthesis of the high-silica LTA framework with two OSDAs.<sup>58–60</sup> In this framework, one of the OSDAs directs the formation of the *sod* cage, whereas the other crystallizes the *lta* cavity. In general, tetramethylammonium is used to crystallize the former, and another template is used to crystallize the latter. Although the dual-OSDA approach does not always lead to product frameworks matching this intuition,<sup>61</sup> the analogy may be combined with the shape descriptors to rationalize the selection of other synthesis routes.

One zeolite that could be of commercial interest in its high-silica form is the KFI framework. The synthetic form of this

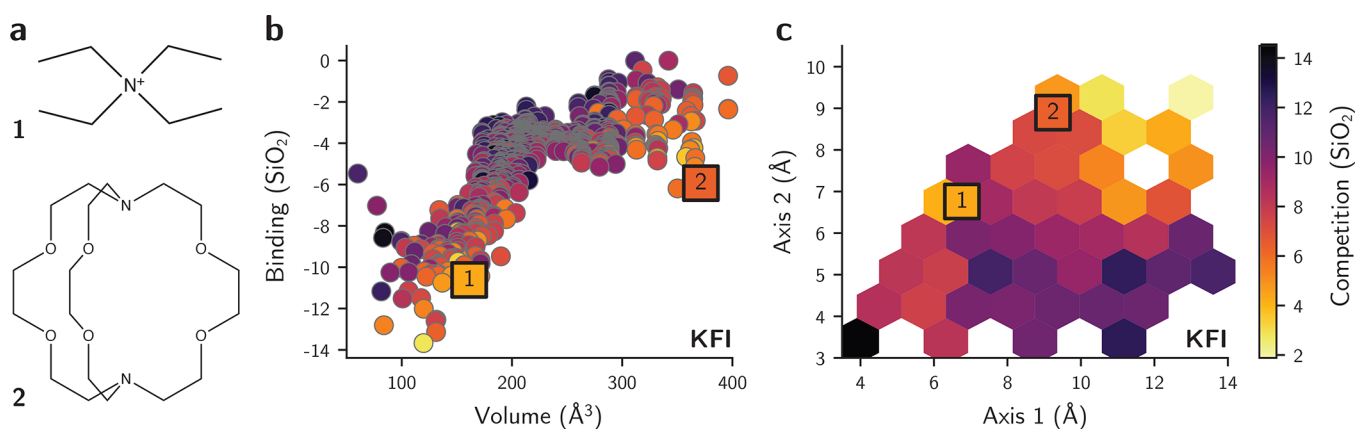


**Figure 6.** a, OSDAs proposed to crystallize the KFI zeolite in a dual-OSDA approach. Each of the OSDAs targets one cavity in the KFI framework and has different b, volumes and c, shapes.

material is usually synthesized with methylated diquaternized DABCO or the 18-crown-6 ether but only in low Si/Al ratios.<sup>47</sup> This has hindered a broader application of KFI for catalysis, and to our knowledge, no synthesis route for KFI with a high Si/Al ratio has yet been reported. To propose a route for crystallization of the KFI zeolite with a dual-OSDA approach, we analyzed the binding energies of OSDAs from the literature toward this material. Figure 6 shows how the use of two distinct OSDAs for the synthesis of KFI can be derived from the binding and shape metrics. In particular, we propose that in addition to selecting an OSDA for crystallizing the *lta* cage, tetraethylammonium may help in directing the formation of the KFI zeolite. This is evidenced by the two binding energy minima in Figure 6b and by the two low-competition regions in the shape space of Figure 6c. Similar to the dual OSDA approach of LTA (Figure S110c), tetraethylammonium is a low-cost template that is selective toward the *pau* cavity present in KFI (Figure S110a,b). This is further supported by the binding energy curve of the MER zeolite, which is formed mostly by the *pau* building unit and has tetraethylammonium as one of its ideal molecules in terms of volume and shape (Figure S110d). Experimental results have also shown that tetraethylammonium OSDAs are located in these *pau* cavities in the synthesis of KFI with multi-inorganic cations, although only with low Si/Al ratios.<sup>62</sup> Although quantifying phase competition within dual-OSDA scenarios with a single figure of merit for OSDA combinations has not been demonstrated yet, decomposing the OSDA design into steps, as allowed by the shape and volume metrics, may help in achieving zeolites with a diversity of cavities and functions.

**Discussion.** This work shows how existing OSDAs may be applied to the synthesis of diverse zeolites not previously associated with them, based on binding, volume, and shape arguments. This “repurposing” strategy has been empirically used in the field for decades, as best exemplified by templates such as tetraethylammonium. This OSDA is known to yield a variety of frameworks in numerous conditions, making these syntheses attractive due to smaller costs of the template.<sup>63</sup> Another example of this computational repurposing strategy is the use of 6-azaspiro[5.6]dodecan-6-ium in the synthesis of CHA. Although the low selectivity of this template had been taken as a drawback in the past,<sup>64</sup> its ability to direct the formation of more than one framework was used as a feature to direct the synthesis of SSZ-13 while also controlling its aluminum distribution.<sup>28</sup>

The strategy in this work is backed by retrospective analysis of literature data and has supported experimental validation in recent works.<sup>28</sup> Nevertheless, improving some of the approximations may lead to even more accurate and predictive models. For instance, it is still unclear whether a small set of simple molecular descriptors can predict all phases arising from zeolite synthesis. “True negative” data points in zeolite synthesis are rarely established due to the dimensionality of synthesis conditions beyond organic templates. For example, combinations of inorganic structure-directing agents have a major influence in the crystallized zeolites<sup>65</sup> and may enable the control of new topologies or compositions.<sup>66</sup> Similarly, residual inorganic cations from the OSDA synthesis can also drive the formation of competing phases.<sup>67</sup> Differences in the intrinsic stability of zeolite frameworks can also play a role during nucleation and growth of zeolites, potentially influencing the outcome of the synthesis. Future predictions may benefit from the simulation of phase selectivity during these kinetic processes,<sup>68,69</sup> enabling a better understanding of the crystallization mechanism beyond host–guest interactions. Finally, heteroatom distributions and concentration can also change the free energy of frameworks<sup>70,71</sup> and affect the final phase selectivity of templates.<sup>72</sup> Therefore, the limits of repurposing approaches have still to be determined both from experimental and theoretical investigations.

From the computational side, the lack of electrostatics, heteroatoms, or inorganic structure-directing agents in the methods from this work only enable a first selection of OSDAs according to their templating effects from shape-matching. Once good templates are selected, more expensive calculations can be performed to understand heteroatom distributions, kinetics of crystallization, or framework stability. Because this work relies on classical force fields as a first layer of simulation, limitations in the force field parametrization may result in errors, such as poor estimates of guest–guest interactions or zeolite formation enthalpies.<sup>35</sup> These may bias the predicted OSDA loadings and host stabilization energies. Although correlations between zeolite synthetic accessibility and OSDA descriptors have been derived using the approximations shown in this work,<sup>28</sup> new computational methods are required to accelerate predictions of electrostatic effects in templated zeolite synthesis at scale.

Even with qualitative design rules, however, computational modeling can provide flexibility in the selection of templates for zeolite synthesis. The dual-OSDA rationalization from



shape and volume descriptors shows how the geometric metrics enable OSDA design even in the absence of simulations. Similarly, the selectivity maps can show how phase competition can be controlled by designing templates with different shapes, which is also useful for the synthesis of intergrown frameworks,<sup>45</sup> or for rationalizing low shape selectivity in the synthesis of large- and extra large-pore zeolites. By abstracting away the complexity of molecular conformation, aggregation, and docking in zeolite synthesis, it is possible to bypass computational simulations when designing templates without sacrificing the intuition behind each descriptor.

## CONCLUSION

In summary, we analyzed a data set of binding energies to repurpose known OSDAs for the synthesis of over 100 zeolites. The data-driven analysis shows that a combination of binding metrics and geometric descriptors of templates may help in the selection of OSDAs that are good binders toward the structures of interest. The data also shows that selectivity maps can be constructed for selected small- and medium-pore zeolites, where frameworks exhibit higher shape selectivity in the templated synthesis. On the other hand, large-pore frameworks seem to have lower shape selectivity due to larger openings. Furthermore, the binding-volume plots may help in the selection of OSDAs for zeolites in a dual-template approach. Using the case of the LTA zeolite as a reference, we propose the use of tetraethylammonium for the synthesis of KFI, aiding the crystallization of its *pau* cages. This work provides examples of alternative OSDAs for several zeolites in the literature and may be a comprehensive reference for future experimental attempts in the synthesis of frameworks with different compositions or synthesis routes.

## DATA AND SOFTWARE AVAILABILITY

The simulation data used in this work is available in ref 28. All templates, zeolites, and metrics are available as interactive figures at <https://zeodb.mit.edu>. The code used to reproduce the plots in this work is available at <https://github.com/learningmatter-mit/Zeolite-Repurposing-Templates> (persistent link at ref 73).

## ASSOCIATED CONTENT

### Supporting Information

The Supporting Information is available free of charge at <https://pubs.acs.org/doi/10.1021/acs.chemmater.2c00064>.

Repurposed OSDAs, binding energies, and shape space for 109 zeolites and illustration of dual-OSDA approach (PDF)

## AUTHOR INFORMATION

### Corresponding Author

Rafael Gómez-Bombarelli – Department of Materials Science and Engineering, Massachusetts Institute of Technology, Cambridge, Massachusetts 02139, United States; [orcid.org/0000-0002-9495-8599](https://orcid.org/0000-0002-9495-8599); Email: [rafagb@mit.edu](mailto:rafagb@mit.edu)

### Authors

Daniel Schwalbe-Koda – Department of Materials Science and Engineering, Massachusetts Institute of Technology,

Cambridge, Massachusetts 02139, United States;

[orcid.org/0000-0001-9176-0854](https://orcid.org/0000-0001-9176-0854)

Omar A. Santiago-Reyes – Department of Materials Science and Engineering, Massachusetts Institute of Technology, Cambridge, Massachusetts 02139, United States;

[orcid.org/0000-0002-0085-874X](https://orcid.org/0000-0002-0085-874X)

Avelino Corma – Instituto de Tecnología Química, Universitat Politècnica de València-Consejo Superior de Investigaciones Científicas, 46022 Valencia, Spain; [orcid.org/0000-0002-2232-3527](https://orcid.org/0000-0002-2232-3527)

Yuriy Román-Leshkov – Department of Chemical Engineering, Massachusetts Institute of Technology, Cambridge, Massachusetts 02139, United States;

[orcid.org/0000-0002-0025-4233](https://orcid.org/0000-0002-0025-4233)

Manuel Moliner – Instituto de Tecnología Química, Universitat Politècnica de València-Consejo Superior de Investigaciones Científicas, 46022 Valencia, Spain;

[orcid.org/0000-0002-5440-716X](https://orcid.org/0000-0002-5440-716X)

Complete contact information is available at:

<https://pubs.acs.org/10.1021/acs.chemmater.2c00064>

## Notes

The authors declare no competing financial interest.

## ACKNOWLEDGMENTS

This work was supported by the MIT Energy Initiative (MITEI) and MIT International Science and Technology Initiatives (MISTI) Seed Funds. D.S.-K. was additionally funded by the MIT Energy Fellowship. The authors acknowledge CSIC for the support through the I-link+ Program (LINKA20381). Computer calculations were executed at the Massachusetts Green High-Performance Computing Center with support from MIT Research Computing.

## REFERENCES

- (1) Davis, M. E. Ordered porous materials for emerging applications. *Nature* **2002**, *417*, 813–821.
- (2) Vermeiren, W.; Gilson, J.-P. Impact of Zeolites on the Petroleum and Petrochemical Industry. *Top. Catal.* **2009**, *52*, 1131–1161.
- (3) Li, Y.; Yu, J. Emerging applications of zeolites in catalysis, separation and host–guest assembly. *Nature Reviews Materials* **2021**, *6*, 1156–1174.
- (4) Li, Y.; Li, L.; Yu, J. Applications of Zeolites in Sustainable Chemistry. *Chem.* **2017**, *3*, 928–949.
- (5) Moliner, M.; Rey, F.; Corma, A. Towards the Rational Design of Efficient Organic Structure-Directing Agents for Zeolite Synthesis. *Angew. Chem., Int. Ed.* **2013**, *52*, 13880–13889.
- (6) Lin, L.-C.; Berger, A. H.; Martin, R. L.; Kim, J.; Swisher, J. A.; Jariwala, K.; Rycroft, C. H.; Bhowm, A. S.; Deem, M. W.; Haranczyk, M.; Smit, B. In silico screening of carbon-capture materials. *Nat. Mater.* **2012**, *11*, 633–641.
- (7) Bai, P.; Jeon, M. Y.; Ren, L.; Knight, C.; Deem, M. W.; Tsapatsis, M.; Siepmann, J. I. Discovery of optimal zeolites for challenging separations and chemical transformations using predictive materials modeling. *Nat. Commun.* **2015**, *6*, 5912.
- (8) Gallego, E. M.; Portilla, M. T.; Paris, C.; León-Escamilla, A.; Boronat, M.; Moliner, M.; Corma, A. Ab initio synthesis of zeolites for preestablished catalytic reactions. *Science* **2017**, *355*, 1051–1054.
- (9) Cundy, C. S.; Cox, P. A. The hydrothermal synthesis of zeolites: History and development from the earliest days to the present time. *Chem. Rev.* **2003**, *103*, 663–701.
- (10) Cundy, C. S.; Cox, P. A. The hydrothermal synthesis of zeolites: Precursors, intermediates and reaction mechanism. *Micro-porous Mesoporous Mater.* **2005**, *82*, 1–78.

- (11) Lobo, R. F.; Zones, S. I.; Davis, M. E. Structure-direction in zeolite synthesis. *Journal of Inclusion Phenomena and Molecular Recognition in Chemistry* **1995**, *21*, 47–78.
- (12) Xie, B.; Song, J.; Ren, L.; Ji, Y.; Li, J.; Xiao, F.-S. Organotemplate-Free and Fast Route for Synthesizing Beta Zeolite. *Chem. Mater.* **2008**, *20*, 4533–4535.
- (13) Maldonado, M.; Oleksiak, M. D.; Chinta, S.; Rimer, J. D. Controlling crystal polymorphism in organic-free synthesis of Na-zeolites. *J. Am. Chem. Soc.* **2013**, *135*, 2641–2652.
- (14) Goel, S.; Zones, S. I.; Iglesia, E. Synthesis of Zeolites via Interzeolite Transformations without Organic Structure-Directing Agents. *Chem. Mater.* **2015**, *27*, 2056–2066.
- (15) Itabashi, K.; Kamimura, Y.; Iyoki, K.; Shimojima, A.; Okubo, T. A Working Hypothesis for Broadening Framework Types of Zeolites in Seed-Assisted Synthesis without Organic Structure-Directing Agent. *J. Am. Chem. Soc.* **2012**, *134*, 11542–11549.
- (16) Schwalbe-Koda, D.; Jensen, Z.; Olivetti, E.; Gómez-Bombarelli, R. Graph similarity drives zeolite diffusionless transformations and intergrowth. *Nat. Mater.* **2019**, *18*, 1177–1181.
- (17) Li, J.; Corma, A.; Yu, J. Synthesis of new zeolite structures. *Chem. Soc. Rev.* **2015**, *44*, 7112–7127.
- (18) Lewis, D. W.; Freeman, C. M.; Catlow, C. R. A. Predicting the templating ability of organic additives for the synthesis of microporous materials. *J. Phys. Chem.* **1995**, *99*, 11194–11202.
- (19) Sastre, G.; Cantin, A.; Diaz-Cabañas, M. J.; Corma, A. Searching Organic Structure Directing Agents for the Synthesis of Specific Zeolitic Structures: An Experimentally Tested Computational Study. *Chem. Mater.* **2005**, *17*, 545–552.
- (20) Pophale, R.; Daeyaert, F.; Deem, M. W. Computational prediction of chemically synthesizable organic structure directing agents for zeolites. *Journal of Materials Chemistry A* **2013**, *1*, 6750–6760.
- (21) Schmidt, J. E.; Deem, M. W.; Lew, C.; Davis, T. M. Computationally-Guided Synthesis of the 8-Ring Zeolite AEI. *Top. Catal.* **2015**, *58*, 410–415.
- (22) Brand, S. K.; Schmidt, J. E.; Deem, M. W.; Daeyaert, F.; Ma, Y.; Terasaki, O.; Orazov, M.; Davis, M. E. Enantiomerically enriched, polycrystalline molecular sieves. *Proc. Natl. Acad. Sci. U.S.A.* **2017**, *114*, 5101–5106.
- (23) León, S.; Sastre, G. Computational Screening of Structure-Directing Agents for the Synthesis of Pure Silica ITE Zeolite. *J. Phys. Chem. Lett.* **2020**, *11*, 6164–6167.
- (24) Muraoka, K.; Chaikittisilp, W.; Okubo, T. Multi-objective de novo molecular design of organic structure-directing agents for zeolites using nature-inspired ant colony optimization. *Chemical Science* **2020**, *11*, 8214–8223.
- (25) Jensen, Z.; Kwon, S.; Schwalbe-Koda, D.; Paris, C.; Gómez-Bombarelli, R.; Román-Leshkov, Y.; Corma, A.; Moliner, M.; Olivetti, E. A. Discovering Relationships between OSDAs and Zeolites through Data Mining and Generative Neural Networks. *ACS Central Science* **2021**, *7*, 858–867.
- (26) Jensen, Z.; Kim, E.; Kwon, S.; Gani, T. Z. H.; Román-Leshkov, Y.; Moliner, M.; Corma, A.; Olivetti, E. A Machine Learning Approach to Zeolite Synthesis Enabled by Automatic Literature Data Extraction. *ACS Central Science* **2019**, *5*, 892–899.
- (27) Bello-Jurado, E.; Schwalbe-Koda, D.; Nero, M.; Paris, C.; Uusimäki, T.; Roman-Leshkov, Y.; Corma, A.; Willhammar, T.; Gomez-Bombarelli, R.; Moliner, M. A Controlling enrichment and DeNO<sub>x</sub> performance of CHA/AEI zeolite intergrowths with ‘a priori’ bi-selective OSDAs. *Angew. Chem. Int. Ed.* **2022**, No. e202201837.
- (28) Schwalbe-Koda, D.; et al. A priori control of zeolite phase competition and intergrowth with high-throughput simulations. *Science* **2021**, *374*, 308–315.
- (29) Burton, A. W.; Lee, G. S.; Zones, S. I. Phase selectivity in the syntheses of cage-based zeolite structures: An investigation of thermodynamic interactions between zeolite hosts and structure directing agents by molecular modeling. *Microporous Mesoporous Mater.* **2006**, *90*, 129–144.
- (30) Zones, S. I.; Burton, A. W.; Lee, G. S.; Olmstead, M. M. A study of piperidinium structure-directing agents in the synthesis of silica molecular sieves under fluoride-based conditions. *J. Am. Chem. Soc.* **2007**, *129*, 9066–9079.
- (31) Schmidt, J. E.; Deem, M. W.; Davis, M. E. Synthesis of a Specified, Silica Molecular Sieve by Using Computationally Predicted Organic Structure-Directing Agents. *Angew. Chem., Int. Ed.* **2014**, *53*, 8372–8374.
- (32) Pushpakom, S.; Iorio, F.; Eyers, P. A.; Escott, K. J.; Hopper, S.; Wells, A.; Doig, A.; Guilliams, T.; Latimer, J.; McNamee, C.; Norris, A.; Sanseau, P.; Cavalla, D.; Pirmohamed, M. Drug repurposing: progress, challenges and recommendations. *Nat. Rev. Drug Discovery* **2019**, *18*, 41–58.
- (33) Baerlocher, Ch.; McCusker, L.B. *Database of Zeolite Structures*. <http://www.iza-structure.org/databases/> (accessed 2022-01-07).
- (34) Sanders, M. J.; Leslie, M.; Catlow, C. R. A. Interatomic potentials for SiO<sub>2</sub>. *J. Chem. Soc., Chem. Commun.* **1984**, 1271–1273.
- (35) Schwalbe-Koda, D.; Gomez-Bombarelli, R. Benchmarking binding energy calculations for organic structure-directing agents in pure-silica zeolites. *J. Chem. Phys.* **2021**, *154*, 174109.
- (36) Landrum, G. RDKit: Open-source cheminformatics. [www.rdkit.org](http://www.rdkit.org) (accessed 2022-01-07).
- (37) Halgren, T. A. Merck molecular force field. I. Basis, form, scope, parameterization, and performance of MMFF94. *J. Comput. Chem.* **1996**, *17*, 490–519.
- (38) Tosco, P.; Stiefl, N.; Landrum, G. Bringing the MMFF force field to the RDKit: implementation and validation. *Journal of Cheminformatics* **2014**, *6*, 37.
- (39) Schwalbe-Koda, D.; Gomez-Bombarelli, R. Supramolecular Recognition in Crystalline Nanocavities Through Monte Carlo and Voronoi Network Algorithms. *J. Phys. Chem. C* **2021**, *125*, 3009–3017.
- (40) Bae, J.; Hong, S. B. Conformation of intrazeolitic choline ions and the framework topology of zeolite hosts. *Chemical Science* **2018**, *9*, 7787–7796.
- (41) Ke, Q.; Khalil, I.; Smeyers, B.; Li, Z.; de Oliveira-Silva, R.; Sels, B.; Sakellariou, D.; Dusselier, M. A Cooperative OSDA Blueprint for Highly Siliceous Faujasite Zeolite Catalysts with Enhanced Acidity Accessibility. *Angew. Chem., Int. Ed.* **2021**, *133*, 24391–24399.
- (42) Gale, J. D. GULP: A computer program for the symmetry-adapted simulation of solids. *Journal of the Chemical Society-Faraday Transactions* **1997**, *93*, 629–637.
- (43) Gale, J. D.; Rohl, A. L. The General Utility Lattice Program (GULP). *Mol. Simul.* **2003**, *29*, 291–341.
- (44) Mayo, S. L.; Olafson, B. D.; Goddard, W. A. DREIDING: A generic force field for molecular simulations. *J. Phys. Chem.* **1990**, *94*, 8897–8909.
- (45) Schwalbe-Koda, D.; Corma, A.; Román-Leshkov, Y.; Moliner, M.; Gómez-Bombarelli, R. Data-Driven Design of Biselective Templates for Intergrowth Zeolites. *J. Phys. Chem. Lett.* **2021**, *12*, 10689–10694.
- (46) Moliner, M.; Martínez, C.; Corma, A. Synthesis Strategies for Preparing Useful Small Pore Zeolites and Zeotypes for Gas Separations and Catalysis. *Chem. Mater.* **2014**, *26*, 246–258.
- (47) Dusselier, M.; Davis, M. E. Small-Pore Zeolites: Synthesis and Catalysis. *Chem. Rev.* **2018**, *118*, 5265–5329.
- (48) Davis, T. M.; Liu, A. T.; Lew, C. M.; Xie, D.; Benin, A. I.; Elomari, S.; Zones, S. I.; Deem, M. W. Computationally Guided Synthesis of SSZ-52: A Zeolite for Engine Exhaust Clean-up. *Chem. Mater.* **2016**, *28*, 708–711.
- (49) Rahimi, N.; Karimzadeh, R. Catalytic cracking of hydrocarbons over modified ZSM-5 zeolites to produce light olefins: A review. *Applied Catalysis A: General* **2011**, *398*, 1–17.
- (50) Martínez, C.; Corma, A. Inorganic molecular sieves: Preparation, modification and industrial application in catalytic processes. *Coord. Chem. Rev.* **2011**, *255*, 1558–1580.
- (51) Bellussi, G.; Millini, R.; Pollesel, P.; Perego, C. Zeolite science and technology at Eni. *New J. Chem.* **2016**, *40*, 4061–4077.

- (52) Maesen, T. L. M.; Schenk, M.; Vlugt, T. J. H.; De Jonge, J. P.; Smit, B. The shape selectivity of paraffin hydroconversion on TON-, MTT-, and AEL-type sieves. *J. Catal.* **1999**, *188*, 403–412.
- (53) Schmidt, J. E.; Xie, D.; Rea, T.; Davis, M. E. CIT-7, a crystalline, molecular sieve with pores bounded by 8 and 10-membered rings. *Chemical Science* **2015**, *6*, 1728–1734.
- (54) Corma, A.; Díaz-Cabañas, M. J.; Jordá, J. L.; Martínez, C.; Moliner, M. High-throughput synthesis and catalytic properties of a molecular sieve with 18- and 10-member rings. *Nature* **2006**, *443*, 842–845.
- (55) Jiang, J.; Yu, J.; Corma, A. Extra-Large-Pore Zeolites: Bridging the Gap between Micro and Mesoporous Structures. *Angew. Chem., Int. Ed.* **2010**, *49*, 3120–3145.
- (56) Burton, A.; Elomari, S.; Chen, C.-Y.; Medrud, R. C.; Chan, I. Y.; Bull, L. M.; Kibby, C.; Harris, T. V.; Zones, S. I.; Vittoratos, E. S. SSZ-53 and SSZ-59: Two Novel Extra-Large Pore Zeolites. *Chemistry – A European Journal* **2003**, *9*, 5737–5748.
- (57) Jiang, J.; Xu, Y.; Cheng, P.; Sun, Q.; Yu, J.; Corma, A.; Xu, R. Investigation of Extra-Large Pore Zeolite Synthesis by a High-Throughput Approach. *Chem. Mater.* **2011**, *23*, 4709–4715.
- (58) Corma, A.; Rey, F.; Rius, J.; Sabater, M. J.; Valencia, S. Supramolecular self-assembled molecules as organic directing agent for synthesis of zeolites. *Nature* **2004**, *431*, 287–290.
- (59) Boal, B. W.; Schmidt, J. E.; Deimund, M. A.; Deem, M. W.; Henling, L. M.; Brand, S. K.; Zones, S. I.; Davis, M. E. Facile Synthesis and Catalysis of Pure-Silica and Heteroatom LTA. *Chem. Mater.* **2015**, *27*, 7774–7779.
- (60) Ryu, T.; Ahn, N. H.; Seo, S.; Cho, J.; Kim, H.; Jo, D.; Park, G. T.; Kim, P. S.; Kim, C. H.; Bruce, E. L.; Wright, P. A.; Nam, I.-S.; Hong, S. B. Fully Copper-Exchanged High-Silica LTA Zeolites as Unrivaled Hydrothermally Stable NH<sub>3</sub>-SCR Catalysts. *Angew. Chem., Int. Ed.* **2017**, *56*, 3256–3260.
- (61) Kumar, M.; Berkson, Z. J.; Clark, R. J.; Shen, Y.; Prisco, N. A.; Zheng, Q.; Zeng, Z.; Zheng, H.; McCusker, L. B.; Palmer, J. C.; Chmelka, B. F.; Rimer, J. D. Crystallization of Mordenite Platelets using Cooperative Organic Structure-Directing Agents. *J. Am. Chem. Soc.* **2019**, *141*, 20155–20165.
- (62) Lee, H.; Shin, J.; Hong, S. B. Tetraethylammonium-mediated zeolite synthesis via a multiple inorganic cation approach. *ACS Materials Letters* **2021**, *3*, 308–312.
- (63) Bello, E.; Ferri, P.; Nero, M.; Willhammar, T.; Millet, I.; Schütze, F. W.; van Tendeloo, L.; Vennestrom, P. N.; Boronat, M.; Corma, A.; Moliner, M. NH<sub>3</sub>-SCR catalysts for heavy-duty diesel vehicles: Preparation of CHA-type zeolites with low-cost templates. *Applied Catalysis B: Environmental* **2022**, *303*, 120928.
- (64) Millini, R.; Carluccio, L.; Frigerio, F.; O’Neil Parker, W.; Bellussi, G. Zeolite synthesis in the presence of azonia-spiro compounds as structure-directing agents. *Microporous Mesoporous Mater.* **1998**, *24*, 199–211.
- (65) Shin, J.; Jo, D.; Hong, S. B. Rediscovery of the Importance of Inorganic Synthesis Parameters in the Search for New Zeolites. *Acc. Chem. Res.* **2019**, *52*, 1419–1427.
- (66) Lee, H.; Shin, J.; Lee, K.; Choi, H. J.; Mayoral, A.; Kang, N. Y.; Hong, S. B. Synthesis of thermally stable SBT and SBS/SBT intergrowth zeolites. *Science* **2021**, *373*, 104–107.
- (67) Du, J.; Yuan, R.; Lin, F.; Liao, L.; Yang, G.; Tao, F.; Cui, Y.; Kirschhock, C. E. Impact of residual sodium cations in azonia-spiro templates on the formation of large and extra-large pore zeolites. *Microporous Mesoporous Mater.* **2022**, *336*, 111891.
- (68) Bertolazzo, A. A.; Dhabal, D.; Molinero, V. Polymorph Selection in Zeolite Synthesis Occurs after Nucleation. *J. Phys. Chem. Lett.* **2022**, *13*, 977–981.
- (69) Bertolazzo, A. A.; Dhabal, D.; Lopes, L. J.; Walker, S. K.; Molinero, V. Unstable and Metastable Mesophases Can Assist in the Nucleation of Porous Crystals. *J. Phys. Chem. C* **2022**, *126*, 3776–3786.
- (70) Muraoka, K.; Chaikittisilp, W.; Okubo, T. Energy Analysis of Aluminosilicate Zeolites with Comprehensive Ranges of Framework

Topologies, Chemical Compositions, and Aluminum Distributions. *J. Am. Chem. Soc.* **2016**, *138*, 6184–6193.

(71) Muraoka, K.; Sada, Y.; Miyazaki, D.; Chaikittisilp, W.; Okubo, T. Linking synthesis and structure descriptors from a large collection of synthetic records of zeolite materials. *Nat. Commun.* **2019**, *10*, 4459.

(72) Schmidt, J. E.; Fu, D.; Deem, M. W.; Weckhuysen, B. M. Template–Framework Interactions in Tetraethylammonium-Directed Zeolite Synthesis. *Angew. Chem., Int. Ed.* **2016**, *55*, 16044–16048.

(73) Schwalbe-Koda, D. learningmatter-mit/Zeolite-Repurposing-Templates: Code for: “Repurposing Templates for Zeolite Synthesis from Simulations and Data Mining” (v1.0). *Zenodo*; 2022. <https://zenodo.org/record/6334746#Yp9u06jMLIU> (accessed 2022-06-07), DOI: 10.5281/zenodo.6334746

## Recommended by ACS

### Data-Driven Design of Biselective Templates for Intergrowth Zeolites

Daniel Schwalbe-Koda, Rafael Gómez-Bombarelli, *et al.*

OCTOBER 28, 2021  
THE JOURNAL OF PHYSICAL CHEMISTRY LETTERS

READ 

### Crystallization of Mordenite Platelets using Cooperative Organic Structure-Directing Agents

Manjesh Kumar, Jeffrey D. Rimer, *et al.*

NOVEMBER 21, 2019  
JOURNAL OF THE AMERICAN CHEMICAL SOCIETY

READ 

### Exfoliated Ferrierite-Related Unilamellar Nanosheets in Solution and Their Use for Preparation of Mixed Zeolite Hierarchical Structures

Wieslaw J. Roth, Andrzej Kowalczyk, *et al.*

JULY 15, 2021  
JOURNAL OF THE AMERICAN CHEMICAL SOCIETY

READ 

### Machine Learning Applied to Zeolite Synthesis: The Missing Link for Realizing High-Throughput Discovery

Manuel Moliner, Avelino Corma, *et al.*

SEPTEMBER 25, 2019  
ACCOUNTS OF CHEMICAL RESEARCH

READ 

Get More Suggestions >